

Short Communication

## A novel $\beta$ -cyclodextrin Functionalized Reduced Graphene Oxide Electrochemical Sensor for Blood Glucose Detection

Lihua Wang<sup>1</sup>, Xiufeng Wang<sup>1</sup>, Ruyi Zheng<sup>2</sup>, Yuan Zhang<sup>1</sup>, Youmei Zi<sup>1</sup> and Yan Huang<sup>1,\*</sup>

1 Department of Hemopathology, The First Affiliated Hospital of Xinxiang Medical College, Xinxiang, 453100, P.R. China

2 The First Clinical Medicine of Xinxiang Medical College, Xinxiang, 453100, P.R. China

#These authors contributed equally to this work.

\*E-mail: [huangyan3123@sina.com](mailto:huangyan3123@sina.com)

Received: 22 October 2017 / Accepted: 10 December 2017 / Published: 28 December 2017

---

The detection of glucose plays a vital role in clinical, biological, and environmental studies. The present work used a facile wet chemical route for the preparation of  $\beta$ -cyclodextrin-functionalized reduced graphene oxide ( $\beta$ -CD/RGO), which was then investigated using Raman spectroscopy, UV-Vis spectroscopy, and FTIR spectroscopy. The corresponding results provided evidence for the effective coverage of  $\beta$ -CD on the surface of RGO. The  $\beta$ -CD/RGO-coated glassy carbon electrode (GCE) showed a low limit of detection (LOD) of 0.4  $\mu$ M, and the linear range was as wide as 1  $\mu$ M - 8 mM. In addition, the successful application of the developed electrochemical biosensor for sensing glucose in blood specimens has been realized.

---

**Keywords:** Blood glucose; Amperometric sensor; Reduced graphene oxide; Electrochemical determination;  $\beta$ -cyclodextrin

### 1. INTRODUCTION

As a chronic clinical condition, diabetes results from elevated glucose levels; the pancreatic  $\beta$  cells responsible for producing insulin to strictly control blood glucose levels malfunction, causing diabetes. Many detrimental conditions may arise due to elevated glucose levels in diabetes patients, including renal, ocular, cardiac, nervous, cerebral and peripheral vascular diseases. As a main health-threatening disease, diabetes could occur in 171 million patients and cause 4 million deaths per year worldwide. An increase of more than double the number of diabetic patients at present has been estimated to occur around the world [1-3]. Currently, diabetes cannot be cured; however, close monitoring of the blood glucose levels of diabetes patients must be guaranteed to prevent possible complications. The preparation of sensitive and accurate apparatuses that sense blood sugar levels for

use in personal care and clinical diagnostics has gained substantial attention, considering the increased need for continuous blood glucose monitoring [4-6]. It is highly essential to develop low-cost, rapid, reliable, sensitive, and selective glucose sensors when also considering the urgent need for developing renewable and sustainable energy, clinical diagnoses, and food and ecological monitoring [7, 8].

A large number of studies investigating methods for sensing glucose have been reported [9, 10]. Techniques used include acoustic [11] and optical [12, 13] sensors, chemiluminescence [1], fluorescent nanogels [14], field effect transistors based on glucose boronic acid chemistry [15], transdermal approaches [16], and near infrared spectroscopy [5, 7]. Nevertheless, the above techniques have some disadvantages, including high cost, design difficulties, and complexity of principles. Fortunately, electrochemical biosensors for sensing glucose have been shown to be an important alternative method due to their great potential for construction and miniaturization of glucose detection apparatuses used for point-of-care applications, resulting in rapid response times, simple operation, low cost, and high sensitivity [2, 17-19] testing.

Typical electrochemical sensors include enzymatic and nonenzymatic types. For glucose sensors of the former type, a glucose-sensitive enzyme that reduces oxygen into hydrogen peroxide under amperometric monitoring is used for the modification of the surface of an electrode [20]. In the latter type, glucose is nonenzymatically sensed via direct electrochemistry of glucose (oxidation or reduction) on varying metal electrodes, particularly using nanomaterials that can enhance the charge transfer between the electrode surface and the reaction via their large surface areas to modify the bare electrode [21, 22]. In previous works, many different nanomaterials have been reported for interdisciplinary applications, i.e., in optoelectronics, electronics, catalysis, and sensing [23, 24]. Features and possible uses could be significantly affected by the nanomaterial phases, sizes, and morphologies, leading to a great focus on the controlled preparation of nanostructured materials with new morphologies [25]. In addition, the distinct properties and structures of the nanomaterials depend on the nanoscale designs of electrode surfaces, which has resulted in many applications of excellent nanomaterials (metal oxides, carbonaceous materials, doped metal oxides, and other nanomaterials and their nanocomposites) to the preparation of glucose sensors [26, 27]. Among the many different types of nanomaterials, metal oxide nanostructures have large surface-to-volume ratios; thus, they are highly sensitive and cost-effective. Additionally, they are also highly selective for coupling with biorecognition molecules with simple designs [28, 29]. Nanostructured metal oxides have many advantages, including improved adsorption capacity, high catalytic efficiency, strong surface reaction activity, modified surface work function, and high surface-to-volume ratios, in addition to electron and phonon confinement, which contribute to their remarkable electrical and optical features. These results confirmed their successful applications in increasing the loading of biomolecules per unit mass of particles, along with the potential of large numbers of novel signal transduction routes in sub-micrometer biosensors [30-32].

As a cyclic oligosaccharide,  $\beta$ -cyclodextrin ( $\beta$ -CD) consists of seven glucose units in a toroidal configuration, and it has a hydrophilic exterior and a hydrophobic inner cavity. It can interact with a large number of organic, inorganic and biological molecules after immobilization on the surface of an electrode via the formation of stable host-guest inclusion complexes [33, 34]. The applications of  $\beta$ -

CD in biosensors for sensing methyl parathion [35], doxorubicin, methotrexate [36], 4-nitrophenol [37], dopamine [38] and imidacloprid [39] have been reported.

The present study presents the synthesis of a  $\beta$ -CD/reduced graphene oxide (RGO) nanohybrid with remarkable dispersity using a facile wet chemical technique. Raman spectroscopy, FTIR, and UV-Vis spectroscopy were used for the characterization of the yielded  $\beta$ -CD/RGO nanohybrid, which was subsequently used to coat a GCE in order to develop a sensitive electrochemical biosensor for sensing glucose. The synergy of  $\beta$ -CD and graphene contributed to the electrochemical improvement of paracetamol using a  $\beta$ -CD/RGO-coated GCE. In addition, the successful application of the developed  $\beta$ -CD/RGO/GCE has been realized for sensing glucose in blood specimens.

## 2. EXPERIMENTS

### 2.1. Chemicals and instrumentation

Graphene oxide (GO) powder was commercially available from JCNANO, INC. Glucose,  $\beta$ -cyclodextrin ( $\beta$ -CD), L-ascorbic acid (99%), 3-hydroxytyramine hydrochloride (DA), paracetamol, uric acid (99%), hydrazine hydrate, and poly(diallyl dimethyl ammonium chloride) (PDDA, 20 wt.%, Mw = 100 000-200 000 g/mol) were commercially available from Sigma-Aldrich. All other reagents were of analytical grade and used without additional purification. For the synthesis of a phosphate buffer solution (PBS), a  $K_2HPO_4$  and  $KH_2PO_4$  solution (0.2 M) was mixed with 18.2 M $\Omega$  cm Milli-Q water with a suitable pH value. All tests used the as-prepared PBS. An OneTouch Ultra Vue glucose detector (LifeScan, China) was purchased as transitional method for glucose detection. The glucose concentration was collected by dropping real sample on the sensor chip. Fourier transform infrared spectroscopy (FTIR, Nicolet iS5, Thermo Scientific, USA) was used to analyze the surface functional groups on the specimens. A UV-Vis spectrophotometer (wavelength range: 190 - 800 nm) was used to obtain optical properties. Raman spectroscopy was carried out with a Raman microscope (Renishaw, inVia; laser light, 514 nm) at ambient temperature.

### 2.2. Preparation of $\beta$ -CD/RGO

Typically, a  $\beta$ -CD/RGO nanohybrid is synthesized by first dispersing GO (10 mg) into water (10 mL) under sonication. This procedure was followed by successive addition of PDDA (1 mL) and  $\beta$ -CD (0.5 g) into the as-prepared GO dispersion. After 120 min of vigorous stirring, the obtained mixture was further mixed with ammonia (500  $\mu$ L) and hydrazine (300  $\mu$ L) and subsequently heated to 90°C, where it was kept for 4 h. After centrifugation, the resulting product was a black precipitate, which was then washed with water three times. The preparation of an RGO control specimen for comparison also followed the above procedure, only PDDA and  $\beta$ -CD were not added.

### 2.3. Glucose detection

A glassy carbon electrode (GCE) was polished with an alumina slurry (0.3 and 0.05  $\mu\text{m}$ ) and was then completely rinsed using ethanol and water. The surface of the electrode was modified by dropping the  $\beta$ -CD/RGO dispersion (5  $\mu\text{L}$ , 0.5 mg/mL) onto the surface of the GCE, followed by drying at ambient temperature. All electrochemical experiments were carried out at ambient temperature using a CHI670E electrochemical workstation. All electrochemical measurements were conducted using traditional three-electrode geometry, where the working, reference, and auxiliary electrodes were a coated GCE, a Ag/AgCl (3 M KCl) electrode, and a platinum wire.

## 3. RESULTS AND DISCUSSION

$\beta$ -CD and PDDA were added to the as-prepared homogeneous GO dispersion, followed by the reduction of GO via hydrazine under an alkaline condition. The dispersity of the  $\beta$ -CD/RGO nanohybrid was enhanced after adding PDDA. The final dispersion was stable for over 30 d. UV-vis spectroscopy results suggested the formation of the nanohybrid. For the GO and  $\beta$ -CD/RGO dispersions, the UV-Vis spectra are shown in Figure 1A. For GO, a typical absorption peak was observed at 227 nm, which suggested the  $\pi \rightarrow \pi^*$  transition of the C=C bonds [40, 41]. A gradual redshift of the aforementioned peak to 265 nm was observed upon the chemical reduction, which indicated that the  $\text{sp}^2$ -carbon network was restored. The structural variations from GO to  $\beta$ -CD/RGO were characterized via Raman spectroscopy. Two different bands were observed at 1352 and 1590  $\text{cm}^{-1}$ , as displayed in the spectrum recorded for GO (Figure 1B), which suggested diamondoid (D) and graphite (G) bands, respectively, where the former band typically indicated that defective graphitic carbon was present, and the latter band corresponded to typical graphitic carbon layers, suggesting the tangential vibration of the carbon atoms [42, 43]. Upon addition of hydrazine, an increase was observed in the intensity ratio of the D and G peaks ( $I_D/I_G$ ) for the  $\beta$ -CD/RGO over a range of 0.877 - 0.958, which suggested that the  $\text{sp}^2$  domains were restored through reduction with hydrazine.

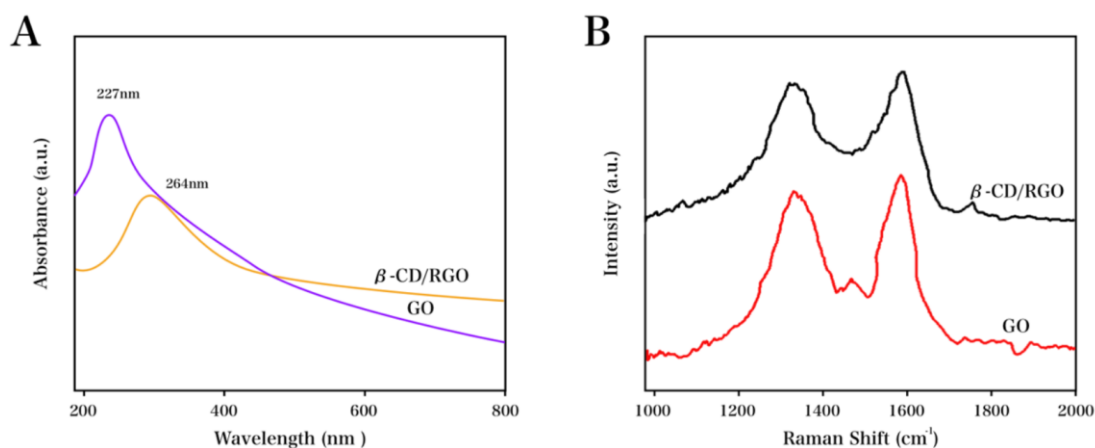


**Figure 1.** (A) UV-Vis spectra and (B) Raman spectra recorded for GO and  $\beta$ -CD/RGO dispersions.

For the graphene sheets, the surface functionalization was studied by FTIR measurement. Figure 2 shows the FTIR spectra of GO,  $\beta$ -CD, PDDA and  $\beta$ -CD/RGO. For GO, peaks at 1713, 1595, 1393 and 1021  $\text{cm}^{-1}$  were observed, which suggested the C=O stretching of COOH groups, C=C vibrations, C—OH stretching vibrations, and C—O vibrations from alkoxy groups, respectively [44, 45]. A remarkable decrease or even disappearance was observed for the aforementioned characteristic peak intensity after hydrazine reduction, which suggested the successful reduction of the GO sheets. In comparison with  $\beta$ -CD,  $\beta$ -CD/RGO showed characteristic  $\beta$ -CD absorption peaks at 2921, 1144, and 1024  $\text{cm}^{-1}$ , suggesting  $\text{CH}_n$  stretching vibrations, O—H bending vibrations, and coupled C—O/C—C stretching, respectively, which confirmed that  $\beta$ -CD was successfully functionalized onto the RGO sheets [46]. Additionally, absorption peaks at 2927, 1482 and 884  $\text{cm}^{-1}$  were observed for  $\beta$ -CD/RGO, suggesting the  $\text{CH}_n$ ,  $\text{CH}_2$  and C—N vibrations of the nitroso groups of PDDA, respectively [47-49], which provided evidence for the fact that PDDA was present. The properties of both PDDA and  $\beta$ -CD were indicated by the spectrum recorded for  $\beta$ -CD/RGO, which suggested the successful functionalization of RGO sheets with PDDA and  $\beta$ -CD.

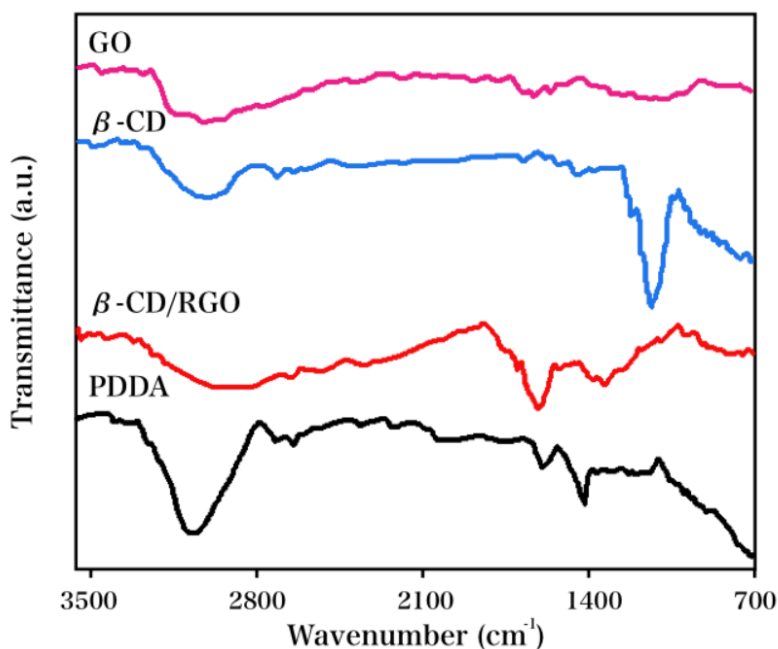


**Figure 2.** FTIR spectra recorded for GO,  $\beta$ -CD, PDDA and  $\beta$ -CD/RGO.

Cyclic voltammograms (CVs) of the RGO-,  $\beta$ -CD-, and  $\beta$ -CD/RGO-coated GCE for the detection of glucose in NaOH are presented in Figure 3A and B. Compared with RGO- and  $\beta$ -CD-coated GCE, the  $\beta$ -CD/RGO-coated GCE showed much larger capacitance (Figure 3A). In addition, the  $\beta$ -CD/RGO-coated electrode was effective in the detection of glucose over a concentration range of 2 - 14 mM. The oxidation current ranged from 0.35 to 0.46 V (Figure 3B). With the increased glucose concentration, a shift to the high potential region was found for the anodic peak. The  $\beta$ -CD/RGO-coated electrode reached a peak current of 977.0  $\mu\text{A}$  in the detection of 12 mM glucose, which was

higher than for the peak current when detecting 14 mM glucose. These results suggested that repetitive experiments with the same electrode showed fatigue or a degradation phenomenon.

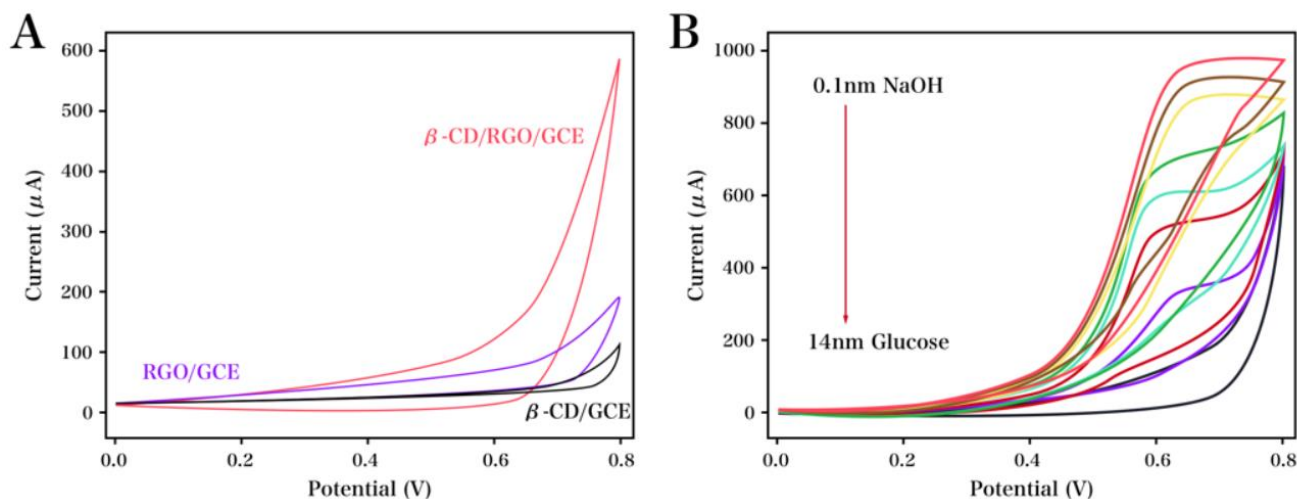


**Figure 3.** (A) CVs recorded for the RGO-,  $\beta$ -CD-, and  $\beta$ -CD/RGO-coated GCE in a 0.1 M NaOH solution. Scan rate: 50 mV/s; (B) CVs recorded for a  $\beta$ -CD/RGO-coated GCE in the presence of glucose at varying concentrations in a 0.1 M NaOH solution. Scan rate: 50 mV/s.

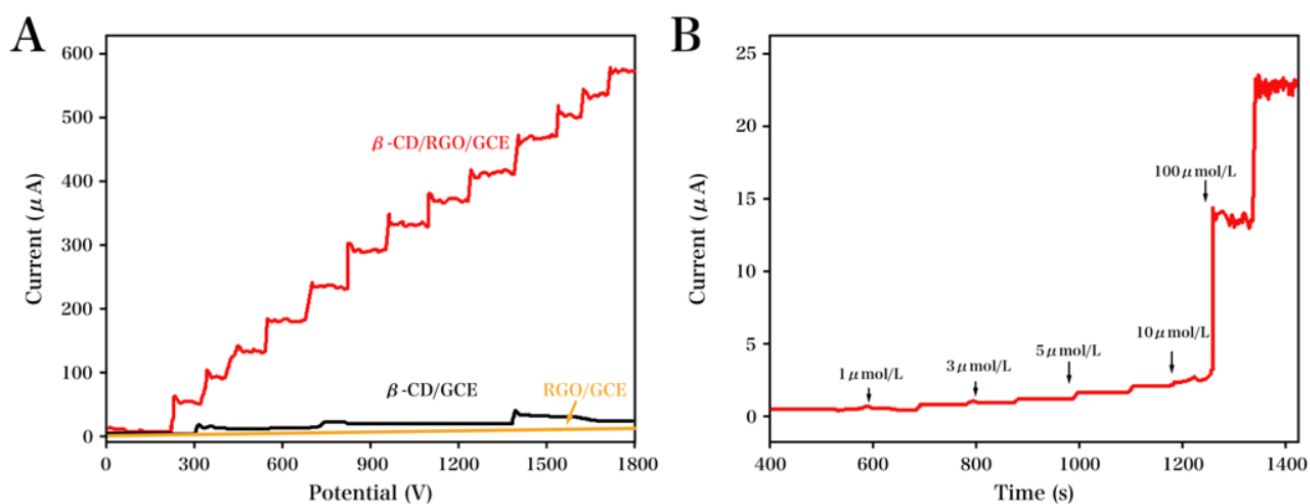


**Figure 4.** (A) Amperometric responses obtained for the RGO-,  $\beta$ -CD-, and  $\beta$ -CD/RGO-coated GCE after adding glucose (0.5 mM) in NaOH solution (0.1 M). (B) Amperometric response obtained for a  $\beta$ -CD/RGO-coated GCE after adding glucose in a 0.1 M NaOH solution.

Figure 4 shows the amperometric responses of different coated electrodes for sensing glucose. For three different coated GCEs, a 0.1 M NaOH solution was mixed with 0.5 mM glucose every 100 s (Figure 4A). At a potential fixed at +0.6 V, the  $\beta$ -CD/RGO-coated GCE showed the best performance in current densities among the three modified GCEs. Figure 4B shows the oxidation currents of the  $\beta$ -CD/RGO-coated electrode (fixed potential, +0.6 V) after varying concentrations of glucose solution

were added to 0.1 M KOH under stirring. The oxidation current was found to be linearly related to the concentration of glucose over a range of 1  $\mu$ M - 8 mM, as shown in the amperometric curve of glucose. The  $\beta$ -CD/RGO-coated electrode showed a low LOD of 0.4  $\mu$ M. It is worth mentioning that the  $\beta$ -CD/RGO-coated GCE exhibits remarkable electrocatalytic performance for glucose detection in terms of the sensitivity, detection limit, and linear range compared with previously reported electrodes, as listed in Table 1. This result is attributed to the high conductivity and large specific surface area of graphene nanosheets.

**Table 1.** Characteristics of comparable electrode material at previously reported glucose sensors.

Electrode	Linear range (mM)	Detection limit ( $\mu$ M)	Reference
NiO/MWCNTs/GCE	0.2-12	160	[50]
Ni(II)-quercetin complex-modified MWCNT ionic liquid paste electrode (Ni(II)-Qu-MWCNT-IL-PE)	0.005-2.8	1	[51]
Ni/poly(o-aminophenol)-modified carbon paste electrode (Ni/POAP/CPE)	0.1-2.7	90	[52]
Nano NiO-modified carbon paste electrode	0.001-0.11	0.16	[53]
Chitosan-reduced graphene oxide-Ni nanoparticle-modified screen-printed electrode (CS-RGO-NiNPs/SPE)	Up to 9	4.1	[54]
$\beta$ -CD/RGO coated electrode	0.001-8	0.4	This work

The  $\beta$ -CD/RGO-coated electrode was used for sensing glucose in blood specimens (collected from a local hospital) to investigate its feasibility. A PBS that contained 0.1 M NaCl (pH 7.4) was used for the dilution of the collected blood specimens. The results are listed in Table 2. During the detection, the standard addition method was used. For the detection of glucose using three blood specimens, the recovery rate ranged from 114.5 to 122.2%, which suggested that the  $\beta$ -CD/RGO-coated electrode could be potentially used for sensing glucose in real specimens. The detection of glucose was also performed with a commercial glucose detector for comparison. As shown in Table 2, the proposed electrochemical sensor produced a comparable result.

**Table 2.** Determination of glucose levels in human serum samples using a  $\beta$ -CD/RGO-coated electrode.

Sample	Found ( $\mu$ M)	Added ( $\mu$ M)	Found ( $\mu$ M)	Recovery (%)	RSD (%)	Glucose detector ( $\mu$ M)
1	4.1	50	62.29	114.5	6.31	61.48
2	12.4	50	76.25	122.2	2.57	73.55
3	5.7	50	62.8	112.7	4.56	61.24

#### 4. CONCLUSIONS

In the present report, a state-of-the-art electrochemical sensor was prepared based on the  $\beta$ -CD/RGO coated GCE for sensing glucose, where a facile wet chemical route was used for the synthesis of  $\beta$ -CD functionalized RGO. The synergy effect of RGO and  $\beta$ -CD contributed to enhancement in the electrochemical property of glucose. Our developed electrochemical biosensor has been applied to the analysis of glucose in blood specimens.

#### References

1. Z. Liu, Y. Guo and C. Dong, *Talanta*, 137 (2015) 87.
2. L. Han, C. Shao, B. Liang and A. Liu, *ACS Applied Materials & Interfaces*, 8 (2016) 13768.
3. S. Gu, K. Ma, J. Kong, K. Al-Ghanim, S. Mahboob, Y. Liu and X. Zhang, *Int. J. Electrochem. Sci.*, 12 (2017) 5092.
4. G. Gao, J. Luo, Z. Ge, S. Chen, S. Chen and H. Yang, *Journal of The Electrochemical Society*, 164 (2017) B189.
5. L. Kang, D. He, L. Bie and P. Jiang, *Sensors and Actuators B: Chemical*, 220 (2015) 888.
6. J. Yang, M. Cho and Y. Lee, *Biosensors and Bioelectronics*, 75 (2016) 15.
7. G. Bharath, R. Madhu, S. Chen, V. Veeramani, A. Balamurugan, D. Mangalaraj, C. Viswanathan and N. Ponpandian, *Journal of Materials Chemistry B*, 3 (2015) 1360.
8. O. Parlak, A. İncel, L. Uzun, A.P. Turner and A. Tiwari, *Biosensors and Bioelectronics*, 89 (2017) 545.
9. C. Chen, Q. Xie, D. Yang, H. Xiao, Y. Fu, Y. Tan and S. Yao, *Rsc Advances*, 3 (2013) 4473.
10. G. Wu, X. Song, Y.-F. Wu, X. Chen, F. Luo and X. Chen, *Talanta*, 105 (2013) 379.
11. X. Wang and X. Zhang, *Electrochimica Acta*, 112 (2013) 774.
12. B. Wang, S. Li, J. Liu and M. Yu, *Materials Research Bulletin*, 49 (2014) 521.
13. D. Zheng, S.K. Vashist, M. Dykas, S. Saha, K. Al-Rubeaan, E. Lam, J. Luong and F. Sheu, *Materials*, 6 (2013) 1011.
14. H. Wang, Q. Lang, L. Li, B. Liang, X. Tang, L. Kong, M. Mascini and A. Liu, *Analytical chemistry*, 85 (2013) 6107.
15. M. Gougis, A. Tabet-Aoul, D. Ma and M. Mohamedi, *Sensors and Actuators B: Chemical*, 193 (2014) 363.
16. Y. Piao, D. Han and T. Seo, *Sensors and Actuators B: Chemical*, 194 (2014) 454.
17. R. Shervedani, M. Karevan and A. Amini, *Sensors and Actuators B: Chemical*, 204 (2014) 783.
18. X. Li, C. Zhao and X. Liu, *Microsystems & Nanoengineering*, 1 (2015) 15014.
19. Z. Yang, Y. Cao, J. Li, Z. Jian, Y. Zhang and X. Hu, *Analytica Chimica Acta*, 871 (2015) 35.
20. H. Yang, G. Gao, F. Teng, W. Liu, S. Chen and Z. Ge, *Journal of The Electrochemical Society*, 161 (2014) B216.
21. V. Goornavar, R. Jeffers, S. Biradar and G. Ramesh, *Materials Science and Engineering: C*, 40 (2014) 299.
22. C. Yang, X. Zhang, G. Lan, L. Chen, M. Chen, Y. Zeng and J. Jiang, *Chinese Chemical Letters*, 25

- (2014) 496.
23. E. Mijowska, M. Onyszko, K. Urbas, M. Aleksandrak, X. Shi, D. Moszyński, K. Penkala, J. Podolski and M. El Fray, *Applied Surface Science*, 355 (2015) 587.
  24. X. Chen, G. Wu, Z. Cai, M. Oyama and X. Chen, *Microchimica Acta*, 181 (2014) 689.
  25. Y. Xing, G. Gao, G. Zhu, J. Gao, Z. Ge and H. Yang, *Journal of The Electrochemical Society*, 161 (2014) B106.
  26. C. Sun, Y. Niu, F. Tong, C. Mao, X. Huang, B. Zhao and J. Shen, *Electrochimica Acta*, 97 (2013) 349.
  27. C. Erdem, D.K. Zeybek, G. Aydoğdu, B. Zeybek, Ş. Pekyardımcı and E. Kılıç, *Artificial Cells, Nanomedicine, and Biotechnology*, 42 (2014) 237.
  28. C. Hsu, F. Su, P. Peng, H. Young, S. Liao and G. Wang, *Sensors and Actuators B: Chemical*, 230 (2016) 559.
  29. C. Li, H. Wang and Y. Yamauchi, *Chemistry-A European Journal*, 19 (2013) 2242.
  30. C. Wei, C. Cheng, J. Zhao, Z. Wang, H. Wu, K. Gu, W. Du and H. Pang, *ChemistryOpen*, 4 (2015) 32.
  31. X. Niu, L. Shi, H. Zhao and M. Lan, *Analytical Methods*, 8 (2016) 1755.
  32. S. Su, H. Cheng and P. Chen, *Journal of the Chinese Chemical Society*, 60 (2013) 1380.
  33. Y. Guo, S. Guo, J. Ren, Y. Zhai, S. Dong and E. Wang, *ACS Nano*, 4 (2010) 4001.
  34. Y. Liu, S. Kang and H. Zhang, *Microchemical Journal*, 70 (2001) 115.
  35. S. Wu, X. Lan, L. Cui, L. Zhang, S. Tao, H. Wang, M. Han, Z. Liu and C. Meng, *Anal. Chim. Acta.*, 699 (2011) 170.
  36. Y. Guo, Y. Chen, Q. Zhao, S. Shuang and C. Dong, *Electroanalysis*, 23 (2011) 2400.
  37. W. Liu, C. Li, Y. Gu, L. Tang, Z. Zhang and M. Yang, *Electroanalysis*, (2013) 2367.
  38. L. Tan, K. Zhou, Y. Zhang, H. Wang, X. Wang, Y. Guo and H. Zhang, *Electrochemistry Communications*, 12 (2010) 557.
  39. M. Chen, Y. Meng, W. Zhang, J. Zhou, J. Xie and G. Diao, *Electrochimica Acta*, 108 (2013) 1.
  40. D. Altuntas, Y. Tepeli and U. Anik, *2D Materials*, 3 (2016) 034001.
  41. J. Xu, X. Cao, J. Xia, S. Gong, Z. Wang and L. Lu, *Analytica Chimica Acta*, 934 (2016) 44.
  42. Z. Shahnava, P. Woi and Y. Alias, *Applied Surface Science*, 379 (2016) 156.
  43. S. ul Haque and M. Naushad, *Enzyme and microbial technology*, 87 (2016) 29.
  44. A. Viinikanoja, J. Kauppila, P. Damlin, M. Suominen and C. Kvarnström, *Physical Chemistry Chemical Physics*, 17 (2015) 12115.
  45. X. Wang, W. Wang, Y. Liu, M. Ren, H. Xiao and X. Liu, *Analytical chemistry*, 88 (2016) 3926.
  46. M. Pfaffeneder-Kmen, F. Bausch, G.n. Trettenhahn and W. Kautek, *The Journal of Physical Chemistry C*, 120 (2015) 15563.
  47. R. Church, K. Hu, G. Magnacca and M. Cerruti, *The Journal of Physical Chemistry C*, 120 (2016) 23207.
  48. W. Guo, J. Chen, S. Sun and Q. Zhou, *The Journal of Physical Chemistry C*, 120 (2016) 7451.
  49. G. Huang, Z. Ni, G. Chen, G. Li and Y. Zhao, *Fullerenes, Nanotubes and Carbon Nanostructures*, 24 (2016) 698.
  50. M. Shamsipur, M. Najafi and M. Hosseini, *Bioelectrochemistry*, 77 (2010) 120.
  51. L. Zheng, J. Zhang and J. Song, *Electrochimica Acta*, 54 (2009) 4559.
  52. R. Ojani, J.B. Raoof and S. Fathi, *Electroanalysis*, 20 (2008) 1825.
  53. Y. Mu, D. Jia, Y. He, Y. Miao and H.-L. Wu, *Biosensors and Bioelectronics*, 26 (2011) 2948.
  54. J. Yang, J. Yu, J.R. Strickler, W. Chang and S. Gunasekaran, *Biosensors and Bioelectronics*, 47 (2013) 530